Molecular Neurobiology (2019) 56:7305–7320
https://doi.org/10.1007/s12035-019-1595-1

RBM15 Modulates the Function of Chromatin Remodeling Factor BAF155 Through RNA Methylation in Developing Cortex

Yuanbin Xie[1,2] · Ricardo Castro-Hernández[1] · Godwin Sokpor[1] · Linh Pham[1] · Ramanathan Narayanan[1,3] · Joachim Rosenbusch[1] · Jochen F. Staiger[1,2] · Tran Tuoc[1,2]

Received: 5 February 2019 / Accepted: 2 April 2019 / Published online: 24 April 2019

Abstract

Chromatin remodeling factor BAF155 is an important regulator of many biological processes. As a core and scaffold subunit of the BAF (SWI/SNF-like) complex, BAF155 is capable of regulating the stability and function of the BAF complex. The spatiotemporal expression of BAF155 during embryogenesis is essential for various aspects of organogenesis, particularly in the brain development. However, our understanding of the mechanisms that regulate the expression and function of BAF155 is limited. Here, we report that RBM15, a subunit of the m6A methyltransferase complex, interacts with BAF155 mRNA and mediates BAF155 mRNA degradation through the mRNA methylation machinery. Ablation of endogenous RBM15 expression in cultured neuronal cells and in the developing cortex augmented the expression of BAF155. Conversely, RBM15 overexpression decreased BAF155 mRNA and protein levels, and perturbed BAF155 functions in vivo, including repression of BAF155-dependent transcriptional activity and delamination of apical radial glial progenitors as a hallmark of basal radial glial progenitor genesis. Furthermore, we demonstrated that the regulation of BAF155 by RBM15 depends on the activity of the mRNA methylation complex core catalytic subunit METTL3. Altogether, our findings reveal a new regulatory avenue that elucidates how BAF complex subunit stoichiometry and functional modulation are achieved in mammalian cells.

Keywords BAF (mSWI/SNF) complex · BAF155 · RNA methylation · RNA decay · RBM15 · METTL3 · Cortical development · Basal progenitor

Introduction

The chromatin remodeler BAF155 is one of the integral subunits of the SWI/SNF-like BAF (Brg1/Brm-associated factor) complex that uses ATP-derived energy to regulate nucleosome occupancy and chromatin architecture. Generally, BAF155 functions as a scaffold protein that participates in the assembly and integrity maintenance of the BAF complex [1–5]. Many recent studies gave an account of the function of BAF155 alone or in synergy with its closely related counterpart the BAF170 subunit [1, 6–8] in orchestrating important cell biological events during development.

At pre-embryonic stages, BAF155 has been reported to play indispensable roles in modulating cell stemness, lineage specification, and transition. It is expressed and incorporated into the embryonic stem cell (esc) BAF complex to regulate pluripotency, proliferation, and survival of ESCs [9–12]. Consistent with its early embryonic expression, BAF155 is reported to be involved in the general development of the body [7, 8, 11, 13–15]. BAF155 has also been reported to be indispensable for olfactory epitheliogenesis during development [8]. Moreover, the preponderance of tumors and cancers due to the lack or insufficiency of BAF155 protein further indicates its importance in maintaining tissue homeostasis and normal development [16–21].

Yuanbin Xie and Ricardo Castro-Hernández contributed equally to this work.

Electronic supplementary material The online version of this article (https://doi.org/10.1007/s12035-019-1595-1) contains supplementary material, which is available to authorized users.

✉ Yuanbin Xie
yuanbin.xie@med.uni-goettingen.de

✉ Tran Tuoc
tran.tuoc@med.uni-goettingen.de

[1] Institute for Neuroanatomy, University Medical Center, Georg-August-University Goettingen, 37075 Goettingen, Germany

[2] DFG Center for Nanoscale Microscopy and Molecular Physiology of the Brain (CNMPB), 37075 Goettingen, Germany

[3] Present address: Laboratory of Systems Neuroscience, Institute for Neuroscience, Department of Health Science and Technology, Swiss Federal Institute of Technology (ETH), 8057 Zurich, Switzerland

Previous findings suggest that dosage of BAF155 expression levels is essential in driving specific developmental processes. For example, whereas BAF155 is known to be highly expressed in ESCs, it is downregulated during differentiation of ESCs to somatic cell lineages such as the neuroectoderm [10, 22]. While knockdown of BAF155 in ESCs promotes expression of other cell lineage markers, the overexpression of BAF155 in somatic cells such as fibroblasts and liver cells enhances the reprograming efficiency of these cell types to the inducible pluripotent stem cells [23–25].

During early brain development, the right dosage of BAF155 is essential for the fidelity of neurulation and for driving normal progression of neural morphogenesis, as the heterozygous loss of BAF155 function in transgenic mouse lines or in de novo mutations in human causes neural tube defects [15, 26, 27]. In the early developing mouse cortex, BAF155 expression is at a low level in apical radial glial progenitors which is reported to promote differentiation of apical progenitors to basal progenitors through cell delamination. However, as corticogenesis advances, BAF155 expression is elevated to reduce such delamination phenomenon and associated genesis of basal progenitors while supporting neuronal differentiation and output [6, 28, 29]. Together, the above findings indicated that the maintenance of the correct spatiotemporal expression of BAF155 is crucial for embryogenesis, particularly for cortical development. Nevertheless, possible upstream factors that regulate the expression of BAF155 in cortical development are not known.

In this current study, we found that the expression levels of the chromatin remodeler BAF155 in mammalian cells is regulated by the RNA-binding motif protein 15 (RBM15)-mediated RNA methylation. Together with METTL3 (methyltransferase-like 3), one of the core catalytic components of the N^6-methyladenosine (m6A) RNA methylation machinery [30, 31], RBM15 regulates BAF155 gene expression by reducing BAF155 mRNA stability, leading to a diminished half-life of BAF155 mRNA. Accordingly, loss of RBM15 caused elevated BAF155 transcript and protein levels, while overexpression of RBM15 decreased the expression level of BAF155. The latter effect resulted in significant loss of BAF155 function in the embryonic mouse cortex, which is similar to the phenotype of our previously reported cortex–specific BAF155 conditional knockout mutants [28], including a defect in establishment of adherens junction (AJ) and abnormal delamination of apical radial glial progenitors.

Results

BAF155 Is a Candidate Target of RBM15-Dependent m6A Regulation in Developing Mouse Cortex

Earlier studies in human cell lines have reported the presence of multiple m6A methylation sites within the sequence of *BAF155* mRNA (two in the last exon and one in exon 6, Fig. 1a, red box) [32]. Recently, three m6A methylation sites were also identified in BAF155 transcripts in developing brain [33]. The RNA localization of m6A reader proteins, including YTHDF1, YTHDF2, YTHDF3, YTHDC1, and YTHDC2, in the abovementioned regions of *BAF155* transcripts was also detected [32–34] and suggests that mRNA methylation may be essential in regulating *BAF155* mRNA metabolism and BAF155 protein turnover.

Alongside the presence of m6A and m6A reader proteins, we examined whether RBM15 and its paralogue RBM15B known to recruit the methyltransferase complex to its target RNAs and control m6A RNA modification [34] participate in the regulation of BAF155 expression. Indeed, individual-nucleotide resolution cross-linking and immunoprecipitation (iCLIP) data obtained from human cell lines shows the presence of small but considerable peaks in occupancy of RBM15 and RBM15B within the *BAF155* transcripts, especially in the vicinity of the methylation sites in exon 6 and near the stop codon (Fig. 1a, red box) [34]. These observations, beside the profound function of BAF155 in the developing cortex, prompted us to investigate whether RBM15 and RBM15B modulate m6A installation to regulate BAF155 expression and function during cortical development.

To compare the expression pattern of RBM15 and BAF155 in the developing cortex, double label immunohistochemistry (IHC) analysis for RBM15 (green) and BAF155 (red) was performed (Fig. 1b). The results revealed their different expression pattern in the developing cortex at E15.5, such that cells in the cortical plate (CP) and intermediate zone (IZ) highly expressing RBM15, exhibit a low expression level of BAF155 (Fig. 1b). In the ventricular and subventricular zones (VZ/SVZ), expression of RBM15 was found in a subset of BAF155+ cells (Fig. 1b, c, filled arrow), as many BAF155+ cells show either low or undetectable expression of RBM15 and vice versa (Fig. 1b, c, empty arrow). This suggests that RBM15 may negatively control the expression of BAF155 via the RNA methylation machinery. Examination of RBM15B expression by RNA in situ hybridization [35] revealed that its expression is virtually absent in the mouse cortex at E14.5 (Fig. S1A). We therefore excluded RBM15B in subsequent investigations in this study.

To validate the binding of RBM15 and the presence of m6A on *BAF155* mRNA from the published iCLIP data, we employed a cultured Neuro2A system. Due to the very low expression level of endogenous BAF155 in Neuro2A cells (our observation, see also Fig. S1E), we therefore transfected the cultured Neuro2A cells with a plasmid containing mouse *BAF155* cDNA. RNA immunoprecipitation (RIP)/quantitative reverse transcription PCR (qPCR) experiments were then performed by using RBM15 and m6A antibodies and the transfected

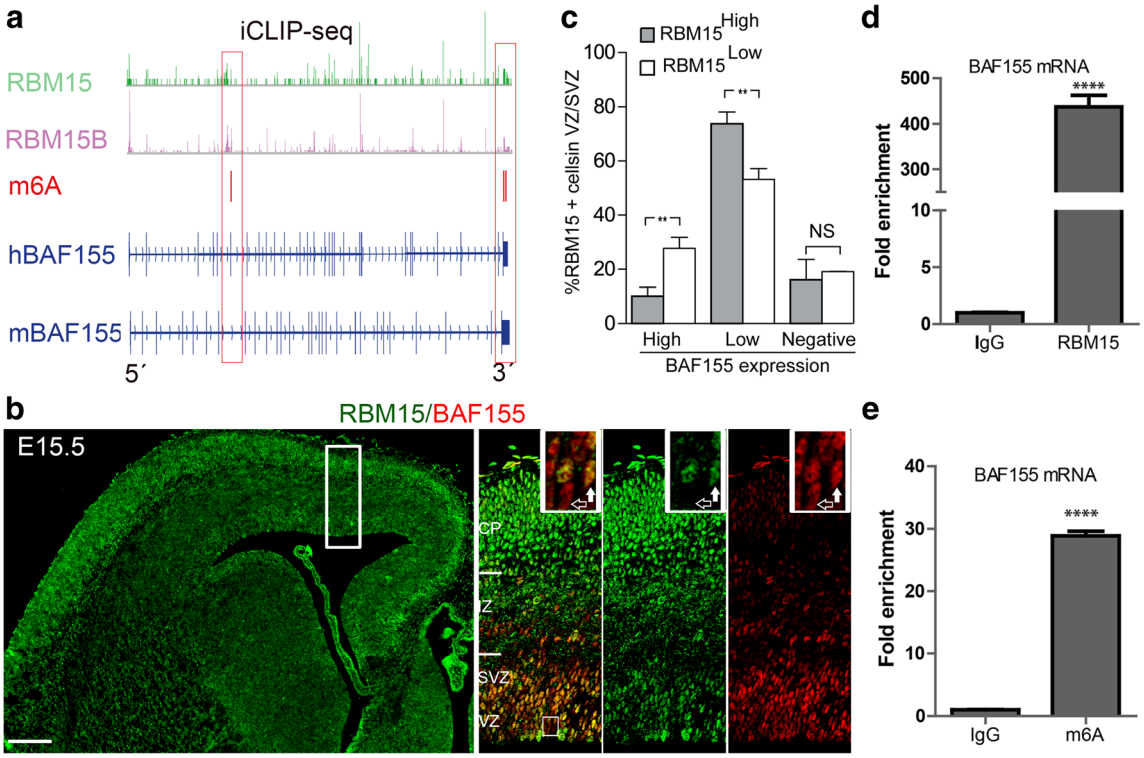

Fig. 1 BAF155 mRNA is a candidate target of RBM15-dependent m6A regulation. **a** Integrated genome browser (IGB) views of RBM15, RMB15B binding, and presence of and m6A along BAF155 gene in mouse and human cells. The occupancy of RBM15 and RBM15B and presence of three m6A sites (one in exon 6 and two near the stop codon) within the BAF155 transcript are indicated in red box. The data is based on the published iCLIP data [32–34, 59]. **b** Double IHC and **c** quantification analyses were performed to compare expression of RBM15 and BAF155 in developing mouse cortex at E15.5. **d** Association of RBM15 with *BAF155* mRNA in RNA immunoprecipitation (RIP) analysis. Plasmids encoding RBM15 and BAF155-Flag were co-transfected into HEK293T cells, RBM15-associated BAF155-Flag mRNA was quantified via qPCR after RIP with RBM15 antibody. IgG was used as RIP control. **e** m6A methylation of *BAF155* mRNA detected by RIP analysis using m6A antibody. Neuro2A cells lysate were used for the RIP, and enrichment of m6A-BAF155mRNA was quantified by q-PCR, and IgG was used as RIP control. VZ, ventricular zone; SVZ, subventricular zone; IZ, intermediate zone; CP, cortical plate. Statistical analyses were done with Student's *t* test. Data are shown as means ± SEM from experimental triplicates. $*p < 0.05$, $**p < 0.01$, $***p < 0.005$, and $****p < 0.001$, $*****p < 0.0005$, $n = 3$. Scale bar = 100 μm

HEK293T cells. To corroborate the binding of RBM15 and the presence of m6A on *BAF155* transcripts as detected in earlier studies (Fig. 1a) [32, 34, 36], we designed a set of primers to target the 5′ end of *BAF155* cDNA in our RIP/qPCR experiments. Compared with the RIP control using IgG, the RIP using RBM15 antibody showed enrichment by more than 420-folds on BAF155 mRNA, confirming the binding of RBM15 protein to BAF155 transcripts (Fig. 1d). The specificity of RBM15 binding to *BAF155 mRNA* was validated by the non-enrichment of the BAF155 counterpart, *BAF170 mRNA*, by RBM15 (Fig. S1B).

Similarly, we detected a strong binding of m6A antibody on methylated mRNA of BAF155 from Neuro2A cells in our RIP/qPCR experiment, indicating that BAF155 mRNA is highly methylated in neuronal cells (Fig. 1e).

Together, the above data suggest that the expression of BAF155 may be regulated by the RBM15-mediated m6A RNA methylation complex.

RBM15 Modulates BAF155 Expression In Vitro

To investigate whether RBM15 regulates BAF155 gene expression, constructs encoding short hairpin RNAs against RBM15 cDNA (shRBM15) were used. The efficiency of shRBM15(s) to knockdown (KD) the expression of exogenous (Fig. S1D) and endogenous RBM15 (Fig. S1E) was examined in the RBM15 cDNA-transfected HEK293T and in mouse Neuro2A cells, respectively. Among five shRBM15 constructs, shRBM15 #1 and shRBM15 #3 effectively knocked down the RBM15 expression in RBM15 cDNA-transfected HEK293T cells (Fig. S1D, lanes: 2, 5). The tested shRBM15 #1 also dramatically reduced endogenous RBM15 protein levels in Neuro2A cells (~ 50%) (Fig. S1E, lane 2).

Given the identified BAF155 mRNA methylation by the RBM15-based m6A RNA methylation complex (Fig. 1), we then sought to determine the effect of RBM15 gene knockdown on the expression level of BAF155 protein. For that

purpose, Neuro2A cells were co-transfected with constructs encoding BAF155-Flag and shRNA control vector or shRBM15 #1. The transfected cells were harvested at 24 h, 48 h, or 72 h post-transfection. The effect of RBM15 knockdown on BAF155-Flag protein levels were examined through Western blotting (WB) analysis, using Flag antibody. As shown in Fig. 2a (lanes 2, 4, 6), co-transfection with shRBM15 #1 markedly increased RBM15-Flag protein band intensity compared with shRNA control vector-transfected cells. Further quantification showed that the shRBM15 #1 augmented BAF155-Flag protein levels by approximately 12.3-folds, 3-folds, and 4.6-folds for 24 h, 48 h, and 72 h co-transfection time points, respectively (Fig. 2b). Moreover, transfection of shRBM15 #3 also dramatically produced 2–11-fold increase in the amount of BAF155-Flag protein in Neuro2A cells, compared with the level from shRNA control vector-transfected cells (Fig. 2c, d; lanes 4, 5, 6). Since the two RBM15 shRNA sequences (#1 and #3) produced similar effect on BAF155 expression, we then used only shRBM15 #1, hereafter simply referred to as shRBM15, for further experiments.

In order to determine the effect of high level of RBM15 expression on BAF155 protein level, we used an in vitro overexpression experimental scheme (Fig. 2e, f). Here, HEK293T cells were transfected with a BAF155-Flag construct together with or without RBM15 expression construct, and WB analysis was performed using Flag antibody to determine the implication of overexpressed-RBM15 on BAF155 protein stoichiometry (Fig. 2e/f). Remarkably, the overexpression of RBM15 resulted in a strong reduction in the protein level of BAF155 by 52–60% when compared with empty vector (EV)-transfected cells (Fig. 2e/f; lanes 2, 4, 6). As expected in our negative control experiment, RBM15 did not occupy BAF170 mRNA (Fig. S1C), also did not affect the expression of BAF170 at the protein level (Fig. S1C).

Given that the full length (FL) RBM15 contains three RNA-binding motifs (RBMs) in the N-terminus, and a Spen paralogue and orthologue domain (SPOC) in the C-terminus (Fig. 2g), we were curious to ascertain which RBM15 domain exerts more relevance in regulating BAF155 expression. To achieve this, HEK293T cells were co-transfected with BAF155-Flag plasmid and constructs lacking either the C-terminus (ΔC, containing RBM domains) or N-terminus (ΔN, containing SPOC domain) of RBM15. BAF155 protein level was then evaluated by WB analysis. It was virtually evident that the full length (FL) of RBM15 protein (Fig. 2h, lane 2) is required to cause reduction in BAF155 protein expression levels since such altered expression of BAF155 was not seen in experiment with either RBM15ΔN or RBM15ΔC (Fig. 2h, lanes 3, 4). Thus, both RBM and SPOC domains are necessary for the full repressive activity of RBM15 on BAF155 protein expression.

Taken together, we have identified RBM15 as a negative regulator of BAF155 protein expression in vitro, with implication of its participation in modulating BAF155 stoichiometry and function in vivo.

Control of BAF155 Expression by RBM15 Depends on mRNA Methylation Machinery

To find out whether RBM15 regulates the *BAF155* mRNA level, BAF155-Flag expression vector was co-transfected with EV or a vector encoding RBM15, and the transfected cells were harvested at 24 h, 48 h, or 72 h post-transfection. BAF155 mRNA levels were analyzed by real-time qPCR (Fig. 3a). Interestingly, overexpression of RBM15 dramatically reduced the BAF155 transcripts by 76–88% (Fig. 3a), indicating that the regulation of BAF155 by RBM15 occurs at the transcriptional or post-transcriptional level. Knowing that RBM15 is a component of the m6A RNA methylation machinery [34], which partly functions in regulating the half-life of target gene transcripts through m6A post-transcription modification, we set out to determine whether RBM15 regulates BAF155 mRNA stability by performing mRNA degradation assay. The transfected HEK293T cells were treated with 5 μM of actinomycin D to block transcription [37]. As expected, overexpression of RBM15 significantly decreased the BAF155 mRNA stability (Fig. 3b). The half-life of BAF155 mRNA was reduced from 22 h in the control experiment (with EV plasmid) to 15.5 h in the RBM15 overexpression experiment (with CMV-RBM15 plasmid) (Fig. 3c). These results indicate that RBM15 negatively controls the BAF155 expression levels via regulating its mRNA stability and decay in vitro.

To further elucidate the extent to which RBM15-mediated repression of BAF155 gene expression depends on activity of the mRNA methylation machinery, we examined the effect of knocking down the core methyltransferase METTL3 or METTL14 of the methylation complex on BAF155 expression. This loss-of-function experiment was done using previously verified shRNA constructs against METTL3 or METTL14 [38]. Expression vectors encoding BAF155-Flag and RBM15 together with shRNA control vector or shRNA targeting mouse METTL3 were co-transfected into Neuro2A cells. Strikingly, shMETTL3 markedly increased the expression of BAF155 (Fig. 3d, e lanes 7–9). Moreover, in the presence of shMETTL3, RBM15 failed to repress the expression of the co-transfected BAF155-Flag vector (Fig. 3d/e, lanes 10–12). In contrast, the co-transfected shRNA targeting human METTL14 did not exert significant repressive effect on either direct (Fig. 3f, g, lanes 7–9) or RBM15-mediated reduction of BAF155

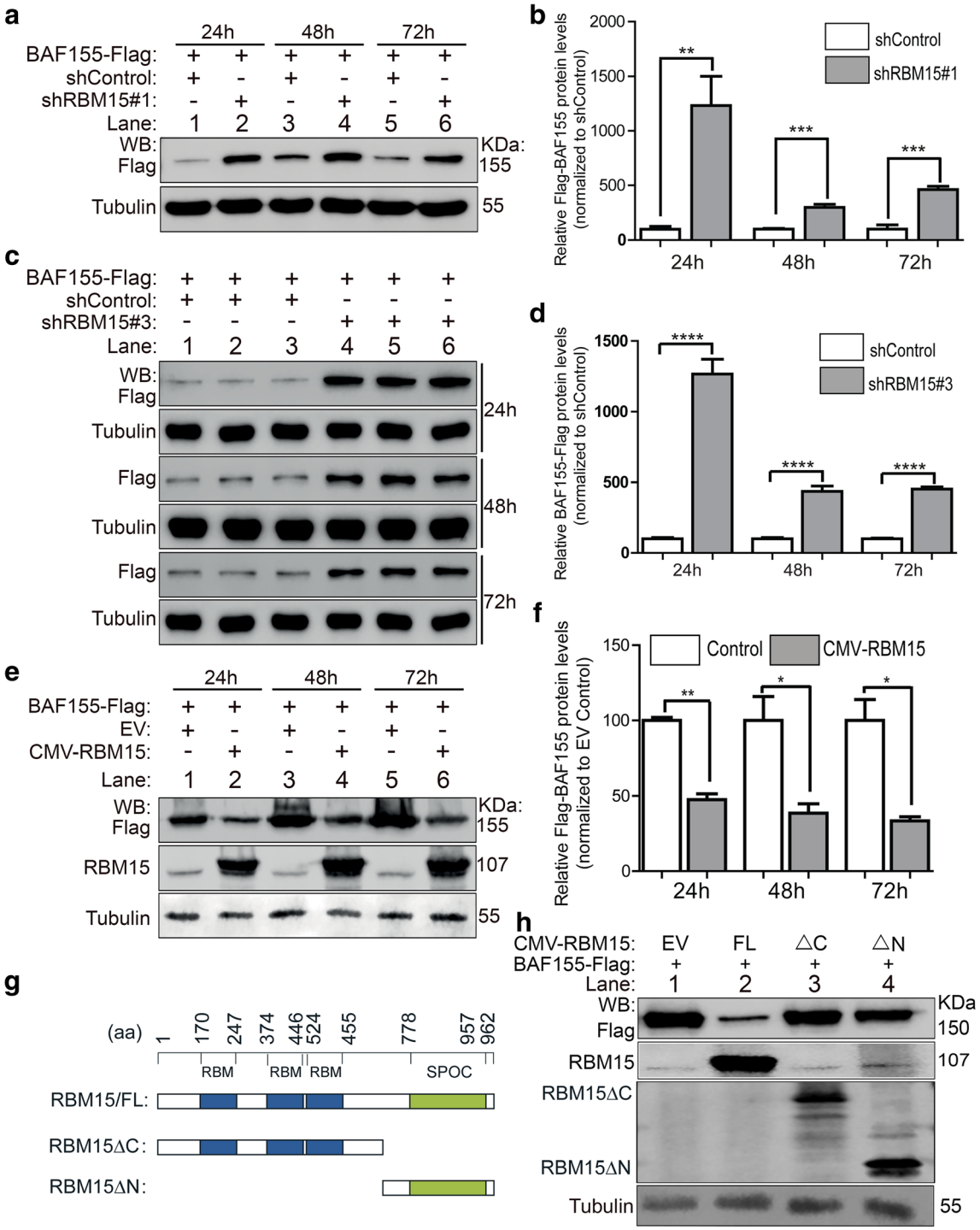

Fig. 2 RBM15 regulates BAF155 protein levels. **a**–**d** Knockdown of RBM15 using shRNAs increased co-transfected BAF155-Flag protein levels in Neuro2A cells. **a**, **c** Western blot (WB) analysis of BAF155-Flag, tubulin was shown as a loading control. **b**, **d** Quantification of the protein band density from A and C, respectively. **e** WB and **f** quantitative analyses revealed that overexpression of RBM15 decreased BAF155-Flag protein levels in HEK293T cells. Plasmids encoding BAF155-Flag, and RBM15 were transfected into HEK293T cells, and protein expression of BAF155-Flag and RBM15 was analyzed by western blot analysis. **g**, **h** Both RBMs and SPOC domains in RBM15 are required for the full repressive activity of RBM15 on BAF155 gene expression. **g** The scheme illustrates the structure of truncated (RBM15 △C, RBM15△N) and full-length (FL) RBM15, which consist of three RNA-binding motifs (RBM, in blue) at N-terminal and a Spen paralogue and orthologue C-terminal domain (SPOC, in green). **h** Expression vectors encoding BAF155-Flag were co-transfected together with or without vectors for RBM15 full-length (FL), RRM domain containing N-terminal (△C)-HA, or SPOC domain-containing C-terminal (△N)-myc into Neuro2A cells. Protein levels of BAF155-Flag, RBM15, △C-HA and △N-myc from Western blot analysis are shown. Tubulin was used as a loading control. Statistical analyses were done with Student's *t* test. Data are shown as means ± SEM from experimental triplicates. $*p < 0.05$, $**p < 0.01$, $***p < 0.005$, $****p < 0.001$, $*****p < 0.0005$, $n = 3$

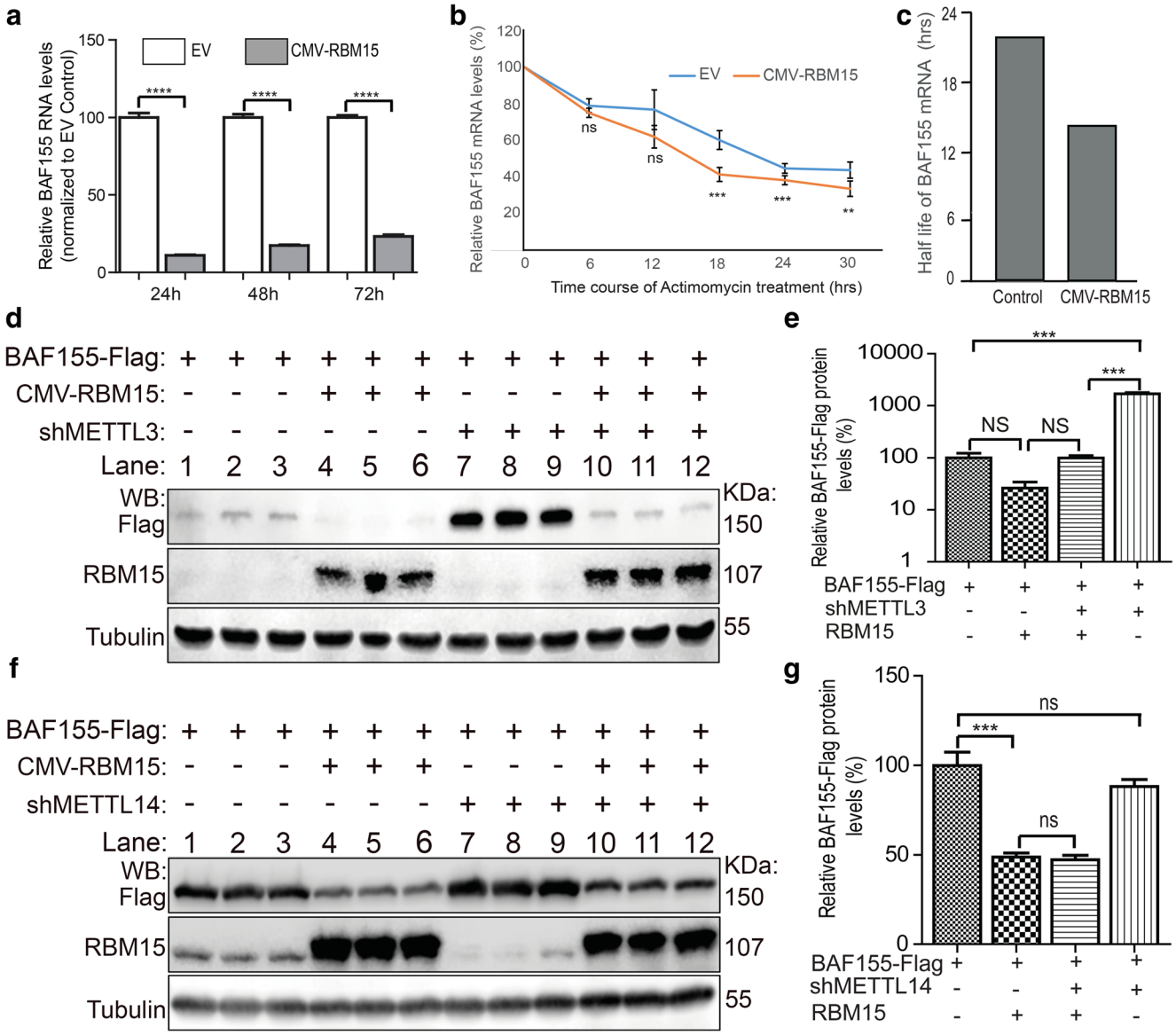

Fig. 3 Regulation of *BAF155* gene expression by RBM15 depends on METTL3. **a** Overexpression of RBM15 reduced *BAF155* mRNA levels. HEK293T cells were transfected with empty vector (EV) or vector encoding BAF155-Flag, RBM15, and pGL3-Basic-Luc as an internal control. mRNA levels of BAF155-Flag were quantified through q-PCR and normalized to the levels of luciferase mRNA from pGL3-Basic-Luc. **b** Overexpression of RBM15 accelerates the degradation of BAF155 mRNA. HEK293T cells were transfected with the abovementioned plasmids. Thirty hour after the transfection, the cells were treated with 5 μM of actinomycin D for the indicated different time. The mRNA levels from RBM15-overexpression group (orange curve) were compared to EV controls (blue curve). **c** Half-life of BAF155 mRNA deduced from B panel. **d** Knockdown of METTL3 released the repression of BAF155 by RBM15. Neuro2A cells were transfected with expression vectors encoding BAF155-Flag, RBM15 with shControl or shMETTL3 as indicated. Protein expression of BAF155-Flag and RBM15 was analyzed by western blot; **e** Quantification of the data from D. The values in *Y* axis are in Log10 scale. **f** Knockdown of METTL14 did not show significant effect on the repressive effect of RBM15 on BAF155 protein level. HEK293T cells were transfected with expression plasmid encoding BAF155-Flag, RBM15 with vectors for shControl or shMETTL14 as indicated. Protein levels of BAF155-Flag and RBM15 were analyzed by western blot. **g** Quantification of the data from panel F. Protein samples are in biological triplicates, and tubulin were used as loading control. Statistical analyses were done with Student's *t* test (in A and B) and one-way ANOVA followed by Bonferroni's multiple comparison test (in E and G). Data are shown as means ± SEM from experimental triplicates. $*p < 0.01$, $**p < 0.001$, $***p < 0.0001$, $n = 3$; ns, not significant

expression at protein level in HEK293T cells (Fig. 3f, g, lanes 10–12). Collectively, the above data suggest that the BAF155-repression capacity of RBM15 requires the functional mediation of the m6A mRNA methylation complex catalytic subunit METTL3 but not METTL14 to effect BAF155 mRNA decay.

RBM15 Regulates Expression of BAF155 in Developing Cortex

To determine whether RBM15 controls the endogenous expression of BAF155 in vivo, E13.5 embryonic mouse brains were co-transfected with either shRBM15 plus GFP plasmids or GFP-only plasmid by means of in utero electroporation (IUE) (Fig. 4a). Cortical sections were collected from both groups 2 days post-electroporation (DPE) and were immunohistochemically examined for BAF155 expression (Fig. 4b). By using ImageJ software, the fluorescence intensities of GFP and BAF155 antibodies staining were estimated in immunomicrographs obtained by confocal microscopy (Fig. 4b). Based on their fluorescence intensity, the GFP+/BAF155+ cells were categorized into three subpopulations. Those with fluorescence intensity signal greater than 30 pixels were designated as highly expressing BAF155 ($BAF155^{high}$, indicated by filled arrows; Fig. 4b, c), whereas those with intensity signal less than 30 pixels were classified as either low expressing or non-expressing/undetectable BAF155 cells ($BAF155^{low}$ or $BAF155^{negative}$, indicated by empty arrows; Fig. 4b, c). We quantified and compared the intensity of fluorescent signals of GFP+/BAF155+ cells in the intermediate zone (IZ) as most of the GFP+ cells translocated into the IZ of shRBM15-injected cortices. Following double immunostaining of BAF155/GFP, we observed that 11.75% ± 4.7 of cells transfected with control (GFP-only) plasmid, were expressing BAF155 at a high level and 73.50% ± 5.4 or 14.75% ± 1.3 showed a low or a negligible BAF155 expression level, respectively (Fig. 4d). However, loss of RBM15 in the cortex treated with shRBM15 + GFP vectors resulted in only 29.72% ± 4.8 of transfected cells displaying the $BAF155^{low}$ feature, while 1.24% ± 2 were $BAF155^{negative}$ cells. We also noticed that BAF155 expression level was substantially elevated in most GFP+/BAF155+ cells treated with shRBM15 plasmid (Fig. 4b, d; filled arrows) as compared to the low expression level of BAF155 in their neighboring non-transfected (GFP negative) cells (Fig. 4b; empty arrows). These results suggest that the stoichiometric level of BAF155 in cortical neural cells is regulated by RBM15 in a cell-autonomous manner. Altogether, these results reveal an in vivo regulatory mechanism in which RBM15 acts cell autonomously to negatively alter the endogenous level of BAF155 in the developing cortex.

To consolidate the inferences derived from our in vivo model system of using RNA silencing to knockdown endogenous levels of RBM15, we studied the effects of RBM15 overexpression (OE). We generated an RBM15 OE construct (RBM15-ires-eGFP), in which expression of RBM15 is under the control of the strongly active CAG promoter, followed by DNA fragments of ires and eGFP (Fig. 3a, S2A). By applying the previously mentioned in vivo electroporation experimental scheme (Fig. 3a), we transfected cortical cells with RBM15 OE plasmid (RBM15-ires-eGFP) and quantified the number of $BAF155^{high}$, $BAF155^{low}$ and $BAF155^{negative}$ cells. We found that overexpression of RBM15 led to diminishing of the $BAF155^{high}$ and $BAF155^{low}$ cell population, but concurrently resulted in an increased number of $BAF155^{negative}$ transfected cortical cells (Fig. 4b, d).

These findings are coherent with the results from the RBM15 gain-, or loss-of-function studies in cultured cells and corroborate the assertion that RBM15 modulates the endogenous protein level of BAF155 in vivo.

RBM15 Controls the Integrity of Ventricular Zone and Delamination of Apical Radial Glia Progenitors Through Regulation of BAF155 Expression in Developing Cortex

Our recent study demonstrated that the deletion of BAF155 in the developing mouse cortex of BAF155cKO mutants causes delamination of apical radial glia progenitors (aRGs) [28]. Given the identified downregulation of BAF155 expression by RBM15 in vivo (Fig. 4), we examined whether RBM15 also controls the BAF155-dependent delamination of aRGs, a phenomenon leading to basal radial glial cell (bRG) generation in the developing cortex [28, 39, 40]. We therefore focused on examining the phenotypic consequence of overexpressing RBM15, which cause the diminished expression of BAF155 in the cortex (Fig. 4). We performed IUE in E13.5 cortex using RBM15-ires-eGFP plasmid to achieve OE of RBM15 in aRGs and their progenies (Fig. 5a, c). The cortical tissue was then harvested 1 DPE and immunostained using GFP, BAF155, SOX2, and PAX6 antibodies. Similar to the diminished expression of BAF155 in IZ after 2 DPE (Fig. 4), overexpression of RBM15 1 DPE caused the decreased expression of BAF155 in aRGs in the VZ (Fig. S2B).

The overexpression of RBM15 also resulted in increased numbers of PAX6+ and SOX2+ RGs in basal cortical regions, including the IZ of RBM15-ires-eGFP-electroporated cortex compared to control plasmid (GFP-only)-injected cortex (Fig. 5a–d, arrows). This observation is coherent with our earlier study in which we found that BAF155 ablation causes ectopic localization of RGs in the cortical IZ [28]. Notably, more GFP negative (−) RGs (Fig. 5a, c; white empty arrows) compared with GFP+ RGs (Fig. 5a, c; filled arrows) were found in the IZ of RBM15-ires-eGFP-transfected cortex (Fig. 5b, d). These results show that RBM15 promotes the delamination of aRGs rather in a cell non-autonomous mode, hence phenocopying BAF155-deficiency in the cortex [28]. Next, we co-transfected both RBM15 and BAF155 expression vectors into E13.5 cortex and examined the cortical phenotype 1 DPE (Fig. 5a). Interestingly, the observed RBM15 overexpression- related phenotype was partly rescued by RBM15 and BAF155 co-expression in the cortex (Fig. 5a–d). This indicates that RBM15 performs a vital function in the

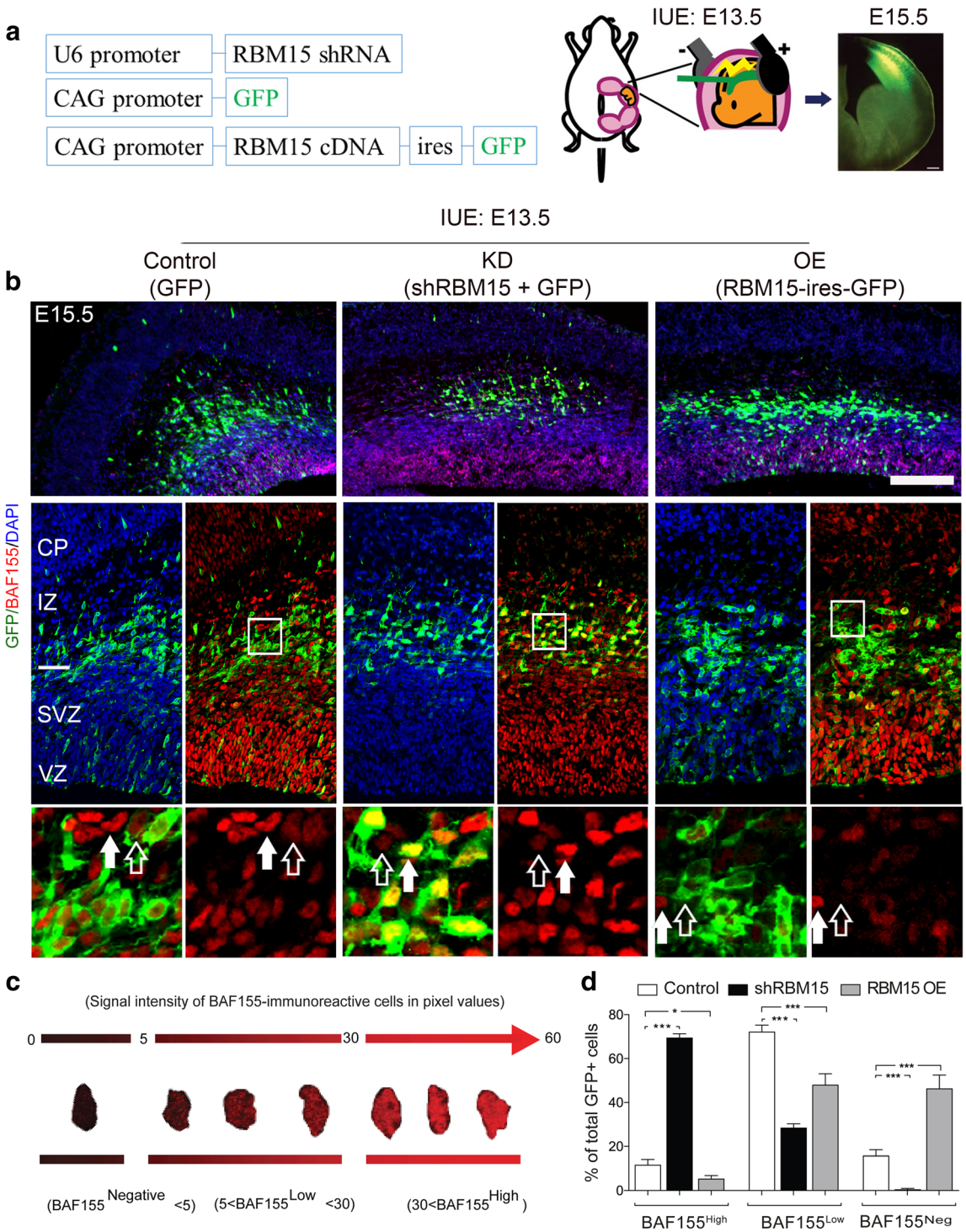

Fig. 4 RBM15 controls expression of BAF155 in developing cortex **a** In utero electroporation (IUE) experiments to knockdown (KD) and overexpression (OE) of RBM15 in developing mouse cortex. shRBM15 (KD), control (GFP) or RBM15-ires-GFP (OE) were electroporated into E13.5 cortices. Embryonic cortices were harvested 2 days later for IHC analysis. **b** Staining of BAF155 protein in E15.5 cortex electroporated at E13.5 with RBM15 OE, KD or control constructs. Insets show the marked increase in BAF155 expression levels in the RBM15 KD cortex, which contrasts with the noticeable reduction in RBM15 OE. **c** After BAF155 immunostaining, the fluorescence intensities were examined microscopically and quantified with ImageJ software. The BAF155+ cells were then classified into three subgroups, namely highly expressing BAF155 ($BAF155^{high}$, intensity of fluorescent signals ≥ 30 pixels), and with a low or undetectable BA155 ($BAF155^{low}$, pixels intensity of fluorescent signals < 30 pixels or intensity of fluorescent signals < 5, respectively; $BAF155^{negative}$, intensity of fluorescent signals ≤ 5 pixels. **d** Quantification of BAF155 intensity categories expressed as the proportion of RBM15 KD- (shRBM15), OE- (RBM15 OE), and shControl-electroporated GFP+ cells. VZ, ventricular zone; SVZ, subventricular zone; IZ, intermediate zone; CP, cortical plate. Statistical analyses were done with one-way ANOVA followed by Bonferroni's multiple comparison test. Data are shown as means ± SEM from experimental triplicates. $*p < 0.01$, $**p < 0.001$, $***p < 0.0001$, $n = 6$; ns, not significant. Scale bar = 100 μm

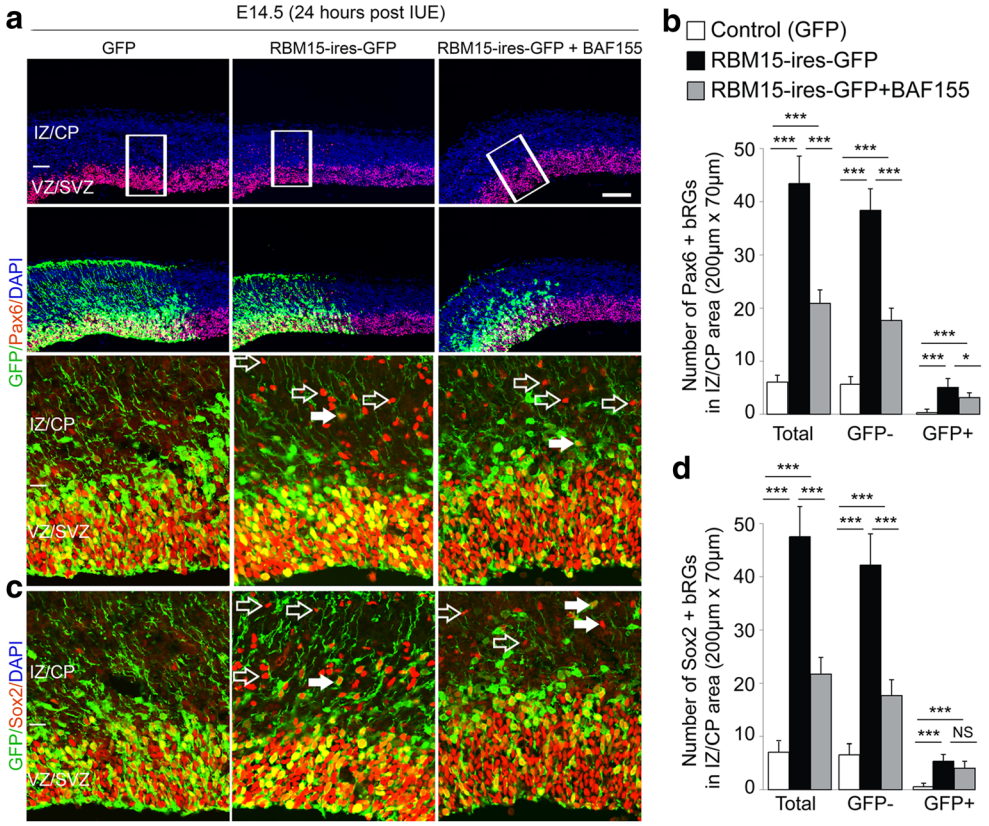

Fig. 5 Diminished expression of BAF155 by RBM15 promotes delamination of aRGs mainly in a cell non-autonomous manner. **a**–**d** Cortical phenotype after overexpression of RBM15 and its rescue by BAF155 co-expression in aRG via in utero (IUE) electroporation. E13.5 cortices were electroporated with the indicated plasmids and collected at 1 day post-electroporation (DPE). Expression of GFP, RG markers: **a** Pax6 and **c** SOX2 were immunohistologically analyzed in coronal brain sections. Statistical analysis indicated that overexpression of RBM15, known to cause diminished expression of BAF155, leads to increased number of **b** Pax6+ RGs and **d** Sox2+ RGs in the IZ/CP. Among the ectopic RGs in IZ/CP, there were significantly higher GFP- (empty arrows in A, C) than GFP+ (filled arrows in A, C) cells. **a**–**d** This cortical phenotype is partly rescued after co-electroporation of both RBM15/BAF155 expression vectors. VZ, ventricular zone; SVZ, subventricular zone; IZ, intermediate zone; CP, cortical plate. Statistical analyses were done with one-way ANOVA followed by Bonferroni's multiple comparison test. Data are shown as means ± SEM from experimental triplicates. $*p < 0.01$, $**p < 0.001$, $***p < 0.0001$, $n = 6$; ns, not significant. Scale bar = 100 µm

delamination of aRGs by specifically modulating BAF155 expression.

In our recent study, we demonstrated that both BAF155 and Pax6 suppress aRGs delamination by regulating the cell adhesion machinery [28]. Since RBM15 modulates the expression of BAF155 (this study), we investigated whether RBM15-mediated regulation of BAF155 expression also affects the transcriptional activity of BAF155/PAX6 direct targets (*Ssx2ip*, *Wnt5a*, *Fgfr1*, *Celsr1*, *Pdgfrb*, *Cdc42ep1*, *and Cdc42ep4*) involved in adherens junction (AJ) establishment or cell-cell interaction. For this, we performed dual-luciferase assay using the promoter region of these genes containing Pax6 binding site(s) [28]. As shown in Fig. 6a, compared with control (Luc + CMV-EV, white bars), co-transfection of Pax6 (Luc + CMV-Pax6, green bars) sufficiently enhanced the luciferase activity. Interestingly, while RBM15 OE reduced Pax6-dependent activation of such promoters (Luc + CMV-Pax6 + CMV-RBM15, red bars), co-transfection of RBM15 and BAF155 expression plasmids significantly restored the promoter activity of the tested target genes (Luc + CMV-Pax6 + CMV-RBM15 + CMV-BAF155, yellow bars). These data imply that RBM15-mediated downregulation of BAF155 expression may influence the promoter activity of AJ/cell-cell interaction genes, thus underscoring the identical cortical phenotypes observed in both BAF155-deficient and RBM15-overexpression cortices.

To consolidate the idea that RBM15-mediated downregulation of BAF155 disrupts the establishment of AJ, we analyzed the expression of AJ markers (ZO1 and α-Catenin) in RBM15-ires-GFP-injected cortex (Fig. 6b–e). Typically, these AJ markers are distinctively expressed at the cortical apical surface (Fig. 6b, d). Consistent with the cortical phenotype in BAF155cKO mutants [28], the expression of ZO1 and α-Catenin in the RBM15-ires-GFP-injected cortical apical surface was noticeably reduced as revealed by fainter fluorescence intensity (Fig. 6b-e, empty arrows in middle panels) as compared to control (GFP)-injected and non-transfected areas (Fig. 6b-e and Fig. 6b, d, filled arrows in left, middle panels).

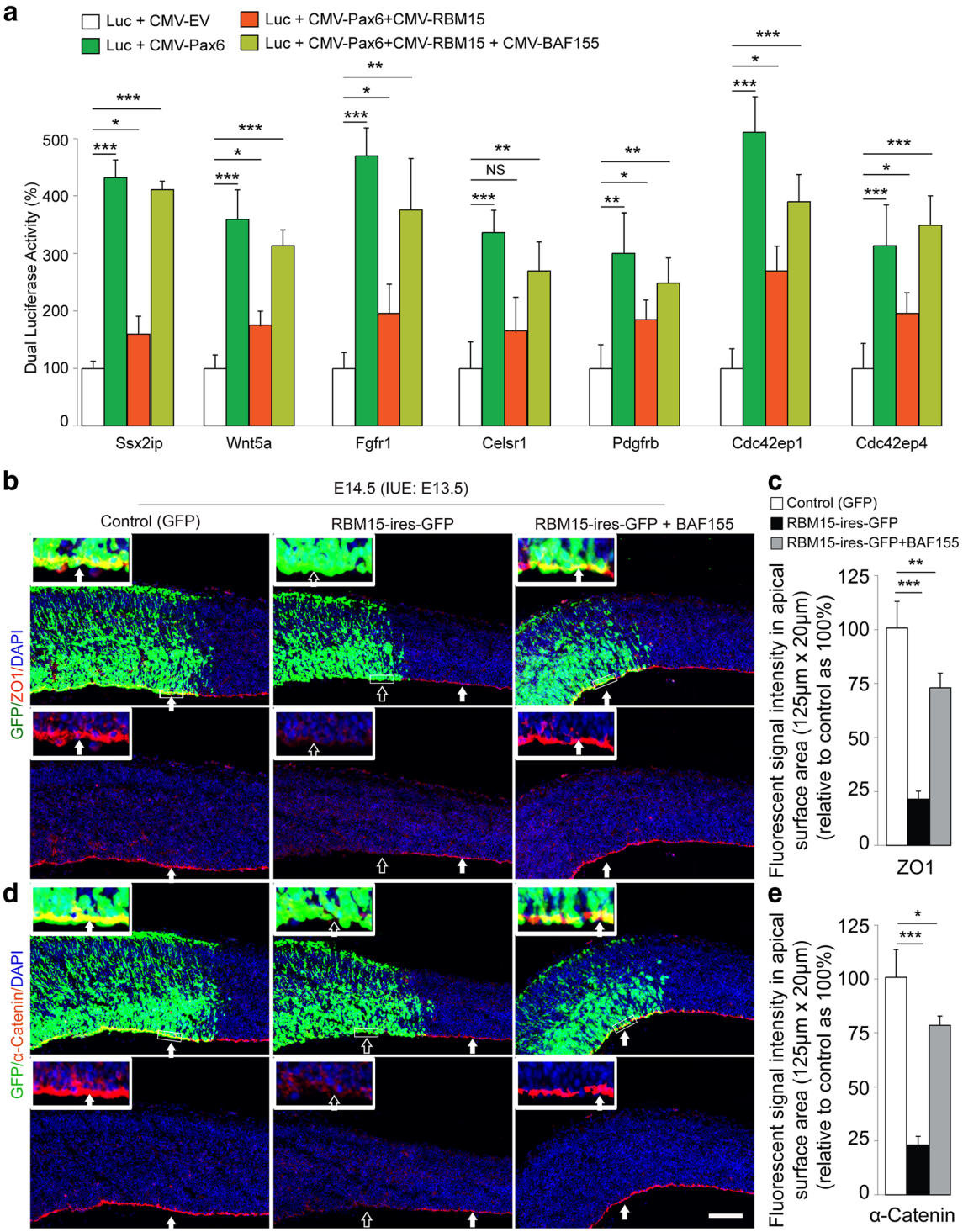

Fig. 6 RBM15 controls the formation of adherens junction by suppressing BAF155 expression. (**a**) Luciferase assay demonstrates that Pax6, BAF155 and RBM15 control transcriptional activity of Pax6/BAF155 target genes. Promoter activities of key genes involved in cell-cell interaction were activated by PAX6 under the Luc + CMV-PAX6 condition in the Luciferase reporter assay. Upon overexpression of RBM15, the promoter activity of these genes was reduced (Luc + CMV-PAX6 + CMV-RBM15 condition). The activity of these genes was however restored in the presence of BAF155 in co-transfection experiment with the BAF155 expression plasmid (Luc + CMV-PAX6 + CMV-RBM15 + CMV-BAF155 condition). (**b**, **d**) Images show immunostaining of ZO1 (**b**) and α-Catenin (**d**) in coronal E14.5 mouse brain sections from the control (GFP-only) plasmids-, RBM15-ires-GFP plasmid-, and RBM15-ires-GFP plus BAF155 plasmids-injected. (**c**, **e**) Quantitative analysis indicated loss of expression of ZO1 and α-Catenin at the ventricular surface of mutant cortex. Statistical analyses were done with One-way ANOVA followed by Bonferroni's multiple comparison test. Values are reported as means ± SEMs. $*p < 0.01$, $**p < 0.001$, $***p < 0.0001$, $n = 6$; ns, not significant. Scale bar = 100 µm

Notably, based on expression of ZO1 and α-Catenin, the formation of AJ appears to be normal when both BAF155 and RBM15 expression plasmids were co-electroporated (Fig. 6b–e and Fig. 6b, d, filled arrows in right panels). This finding suggests that by directly repressing the expression of BAF155 and possibly its downstream target genes, RBM15 is able to regulate the formation of adherens junction belt known to provide anchorage for aRGs in their ventricular zone niche.

Altogether, our data lead us to conclude that the RBM15 subunit of the m6A RNA methyltransferase complex controls the integrity of the ventricular zone and delamination tendency of aRGs, at least in part, by directly regulating the expression of BAF155 in the developing cortex (Fig. 7).

Discussion

While the function of BAF155, a core component of the BAF complex, has been well characterized in cortical development [1, 6, 13, 28, 41], regulatory mechanisms of the gene expression and upstream factors of BAF155 are largely unknown. The concept of RNA methylation has emerged as an essential post-transcriptional regulator of gene expression and developmental processes through regulating the fate of mRNAs in a dynamic manner. In mammals, the reversible installation of methyl marks like m6A on mRNAs alters the epitranscriptomic landscape to influence many cell biological processes including DNA damage repair, X chromosome inactivation, stem cell proliferation and differentiation, tumorigenesis, and stress response [33, 34, 36, 42, 43]. Several previous studies have also suggested that (m6A) RNA methylation is emerging as a principal mechanism adopted by neural cells to regulate their development and function [33, 38, 43–46]. In this study, we observed that RBM15 plays a crucial role in regulating BAF155 gene expression via m6A modification at the post-transcriptional level, leading to modulation of BAF155 gene expression and function to impact cortical development.

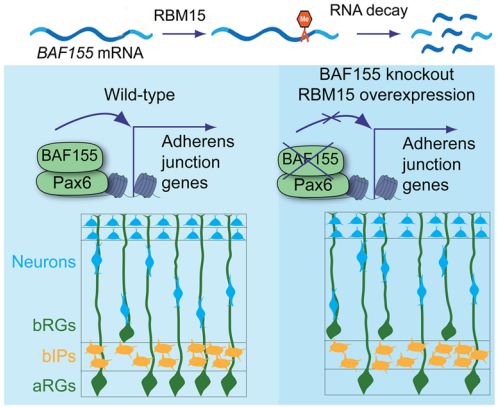

Fig. 7 Scheme illustrating the epitranscriptomic regulation of BAF155 expression by RBM15 in genesis of bRGs in developing cortex. RBM15 promotes m6A (N6-methyladenosine) methylation of BAF155 mRNA, leading to degradation of BAF155 mRNA. By negatively regulating the expression level of BAF155 subunit of the BAF complex, the overexpression of RBM15 is able to cause similar effect as knockout/knockdown of BAF155 in the developing cortex, including suppression of transcriptional activity of Pax6 target genes, which are important for establishment of adherens junction and delamination of cortical progenitors. Whether BRM15 is important for other aspects of cortical development such as genesis of bIP, neuronal migration is under investigation of a separate study. aRGs, apical radial glial progenitors; bIPs, basal intermediate progenitors; bRGs, basal radial glial progenitors

The Emerging Role of RNA Methylation in Neural Development

RBM15 and its paralogue RBM15B have been proposed to bridge the methyltransferase complex to its target RNA, which is critical to control RNA N^6-adenosine methylation, and promoting transcriptional repression [34]. The modification of m6A influences many steps in the mRNA processing cycle, including mRNA splicing, transport from the nucleus to the cytoplasm, degradation, and translation efficiency [30]. Alongside other studies, our present observations reveal that *BAF155* mRNA is a target of the RBM15-based RNA methylation machinery. We have put together several experimental results that argue in favor of this notion. So far, our study shows the first in vivo evidence that RBM15 regulates BAF155 gene function by modulating expression levels through mRNA methylation.

Other studies have reported that METTL3 and METTL14 normally form a stable heterodimer to serve as the m6A installation hub in the mRNA methylation machine [31]. However, both subunits can elicit uniquely different consequences when ablated because METTL3 chiefly performs a catalytic function whereas METTL14 is essential for RNA substrate recognition in the mRNA methylation complex [47]. Another notable reason indicating that METTL3 and METTL14 may affect different targets is their ability to selectively bind to their targets despite having about 56% binding site homology [31]. Interestingly, our study shows that the regulation of BAF155 expression by RBM15 depends on METTL3, but not METTL14. The apparent non-redundant function of METTL3 and METTL14 in RNA methylation was recapitulated in other studies in which it was reported that *Nanog* mRNA expression is downregulated in *Mettl3*-null E6.5 embryos [48], but levels were unaffected by *Mettl14*-null mutation [49]. This provokes the idea that other substrate recognition adaptor proteins other than METTL14 may exist in the RNA methylation complex to cooperate with METTL3 in m6A deposition on mRNAs. A plausible inference from our study is that RBM15 may provide additional or auxiliary function in mRNA substrate recognition of specific targets including BAF155. In any case, further investigations are needed to expound this assertion.

The core m6A RNA methylation complex subunits and associated factors are taking center stage in the epitranscriptomic regulation of mammalian cortical development. Studies have revealed their critical roles in different aspects of cortical neurogenesis. One such key study reported that the conditional knockout (cKO) of METTL3 through Nestin-Cre driver leads to protracted cell cycle of apical neural progenitors and cortical neurogenesis [38]. However, the loss of METTL14 in the METTL14cKO_Nestin-Cre mutants resulted in decreased progenitor proliferation, precocious neuronal differentiation, and diminished number of late-born neurons. In our IUE experiments involving gain- and loss-of-function of RBM15, we observed that majority of GFP+ cells migrated into the IZ upon knockdown of RBM15, whereas many GFP+ cells were retained in VZ after RBM15 overexpression compared with control plasmid-injected cortex (Fig. 4). While cortex-specific RBM15cKO mutants are currently being generated for further studies to consolidate our in vivo findings, observations from the IUE experiment suggest a possible role of RBM15 in aRG proliferation and differentiation. The phenotypic characterization of RBM15 mouse mutants will thus provide additional insight into the biological significance of the m6A RNA methylation machinery in brain development.

RBM15 Acts as an Upstream Factor of BAF155 in Cell Delamination and bRG Genesis

The mammalian brain has undergone evolutionary changes grossly manifested in the sheer size and shape of the cerebral cortex. The radial and tangential expansion of the cortex leading to formation of gyri/sulci is closely associated with the evolution of higher cognitive functions in primates and humans. Pioneering studies have shown that besides basal intermediate progenitor cells (bIPs), a unique type of cortical progenitors, known as basal (or outer) radial glial cells (bRGs) exist to primarily amplify the neurogenic output that underlie cortical expansion in higher mammals [50–53]. Such early investigations have also demonstrated the role of cell-intrinsic determinants of basal progenitor generation [54, 55]. Our studies have shown the specific role of the chromatin remodeling BAF complex in bIPs genesis. The deletion of BAF170, one of the core subunits of BAF complex results in increased production of bIPs from aRGs, at the expense of direct neurogenesis. This results in an expansion of upper neuronal layer and increased cortical surface and thickness [29].

Interestingly, our recent findings indicate that the BAF complex has not only a role in bIP genesis but also bRG genesis [28]. The abrogation of BAF155 results in ectopic distribution of progenitors including bRGs in the cortical IZ. These bRGs not only express RG markers such as PAX6/SOX2 but also display prominent pia-directed basal processes and gene expression profile characteristic of bRGs. One of the prominent findings of this study is that, apart from cell-autonomous functions, BAF155 seems to regulate bRG genesis predominantly via cell non-autonomous mechanisms involving cell-cell interaction and cell adhesion remodeling [28]. We have shown that RBM15 regulates *BAF155* mRNA stability and its stoichiometry to orchestrate progenitor cell delamination at the ventricular surface of the developing forebrain. Such mechanistic approach to bRG genesis by apical progenitor delamination through downregulation of AJ protein at the ventricular surface has also been reported by another recent study [40]. Our co-expression analysis indicated a significant proportion of cortical progenitors expressing a high level of both RBM15 and BAF155. This suggests that this cell population lacks the inhibitory effect of RBM15 on *BAF155* expression. Our future study will investigate whether the negative regulatory effect of RBM15 on gene expression program in developing cortex is dependent on the presence of methyltransferase METTL3 or METTL14 as observed in vitro (Fig. 3d–g). Our current study suggested that RBM15 plays essential role in cortical development. It will be interesting to investigate function of this epitranscription factor in generating different subtypes of cortical progenitors, neurons, and other in aspects of RNA metabolism, including RNA splicing and RNA export.

What then is the rationale for aRGs or their derivatives delaminating to migrate/relocate to basal cortical areas? The essence is to possibly make room for cortical expansion and prevent cellular crowding in the VZ. The cortical ventricular zone is typically tightly packed with a pseudostratified layer of aRGs principally responsible for producing diverse types of basal progenitors, neurons, and glia. During the various stages of cortical development, newborn progenies of aRGs must constantly exit the VZ to facilitate proper cortical layer formation and prevent cells other than aRGs from accumulating in the VZ. The integrity of the VZ is maintained through cell adhesion and cell-cell interactions which tether aRGs in this zone. Meaning, such cell adhesion molecules in the VZ must be subtly regulated to synchronize the rate of cell delamination with stages of cortical development. The findings of this current study indicate a putative mechanism that control cell delamination and integrity of the VZ through RBM15-dependent regulation of BAF155 expression levels in the apical progenitors, thus highlighting the importance of RNA N^6-adenosine methylation in cortical development.

Distinct phenotypes have been ascribed to the amount of BAF155 (i.e., under BAF155 heterozygous, homozygous, or missense mutation conditions) in cortical development [1, 6, 8, 26–28]. It will be interesting for prospective studies to elucidate how the expression of RBM15 is regulated in cortical progenitors and how cells decipher delamination cues in the VZ to elicit alteration in BAF155 expression levels. This will afford further understanding

of the evolutionarily significant process of bRG genesis through cell delamination, a phenomenon known to be more prominent in the primate and human brain.

Methods

Plasmids

Plasmids used in this study: pGL3 basic (Promega); pCIG2-ires-eGFP (gift from Dr. Francois Guillemot, NIMR London; Hand et al. 2005); pNTGFP-RBM15, pcDNA3-HA-N-RBM15 [1-608aa]), and pcDNA3-RBM15-C [635-962aa]-myc were kind gifts from Dr. Diane S. Krause [56]; pCIG2-RBM15 was generated by inserting mouse RBM15 cDNA (PCR-based amplification from pNTGFP-RBM15) into SmaI-digested pCIG2-ires-eGFP vector; BAF155-Flag and Myc-BAF170 were generously provided by Dr. Rho H. Seong [5]; shRBM15 #1 and #2 (corresponding to MSH025627-31 to MSH025627-32 in Genecopoeia); shRBM15 #3 to #5 (gifts from Dr. Diane S. Krause, shRBM15 #3 to #5 were corresponding to the shOOT-IV, shOOT-II, and shOOT-I [56]); pUEG-shMETTL3 and cFUGW-shMETTL14 plasmids were kindly provided by Dr. Hongjun Song [38]; pLuc-Ssx2ip, pLuc-Wnt5a, pLuc-Fgfr1, pLuc-Celsr1, pLuc-Pdgfrb, pLuc-Cdc42ep1, and pLuc-Cdc42ep4 (PCR-based amplification of respective gene promoters from genomic DNA followed by cloning into pGL3 basic, Promega).

Antibodies

The polyclonal (pAb) and monoclonal (mAb) primary antibodies used in this work were purchased from the following commercial sources: BAF155 Mouse IgG (1:20 IHC, Santa Cruz, Sc48350X), betaTubulin (DSHB, E7-s), beta Catenin (1:300, BD Pharmingen, #610153); Flag Mouse IgG (1:1000, Sigma F1804), GFP (1:400, Abcam, #13970); Normal rabbit IgG (CST, 2729S); Pax6 mAb mouse (1:100; Developmental Studies Hybridoma Bank); RBM15 Rabbit IgG (1:50 IHC, Proteintech 10587-1-AP); RBM15 Rabbit IgG (1:20 IHC, 1:2000 WB Sigma HPA019824); Sox2 mouse mAb (1:100; R&D Systems); ZO1 Mouse IgG (1:20 IHC, R26.4C, DSHB); HA Rat IgG (1:1000, WB Roche, 1867423); Myc Mouse IgG (1:1000 WB, CST, 2276S). Secondary antibodies used were IRDye® 680RD goat anti-rabbit IgG (1:15000, LI-COR); IRDye® 680RD goat anti-mouse IgG (1:15000, LI-COR); IRDye® 800CW goat anti-rabbit IgG (1:15000, LI-COR); IRDye® 800CW goat anti-mouse IgG (1:15000, LI-COR); and Alexa 488-, Alexa 568-, Alexa 633-, and Alexa 647-conjugated IgG (various species, 1:400; Molecular Probes).

Cell Cultures, Transfection

HEK293T and Neuro2A cells were cultured in Dulbecco's modified Eagle's medium (DMEM) medium plus 10% FBS. All the transfections were performed using Lipofectamine 2000 (Invitrogen) according to the supplier's protocols. Luciferase activity in cell lysates was quantified using a luciferase assay system (Promega) according to the manufacturer's instructions.

Analysis of the Published iCLIP-Seq Data

iCLIP-seq data are with the following accession numbers: GSE63753 for RBM15 [32] and GSE78030 for m6A [34]. YTHDF1, YTHDF2, YTHDF3, YTHDC1, and YTHDC2 were obtained from published datasets [32–34], aligned to the corresponding reference genome (mm10 or hg19), and visualized using IGV (http://www.broadinstitute.org/igv).

RNA Purification and Real-Time qRT-PCR Analysis

Total RNA was isolated from Neuro2A and HEK293T cells using Trizol Reagent (Gibco), treated with DNaseI and purified with RNA Clean & Concentrator (Zymo Research). cDNA synthesized through ProtoScript first strand cDNA synthesis kit (NEB) were used for SYBR-green–based quantitative real-time PCR. All the primers for qRT-PCR were shown in Table S1.

RBM15 and m6A RNA Immunoprecipitation (RIP)

RBM15 and m6A RNA immunoprecipitations were performed using Magna RIP™ Kit (merckmillipore) according to the manufacturer's instructions. In brief, cells cultured on 10 cm dish were lysed in 400 ul of complete RIP lysis buffer-containing protease inhibitors and RNase inhibitor. RBM15 protein or m6A-modified transcripts were pulled-down by Dynabeads-associated RBM15 antibody or m6A antibody (synaptic systems). A mock pull-down was done with normal rabbit IgG (Cell Signaling Technologies). The immunoprecipitated complex was washed intensively and the pull-down RNA was extracted using Trizol reagent. Purified RNA were treated with DNAse I and used for cDNA thynthesis and qRT-PCR analysis. The dynabeads-associated 18 s RNA was used as internal control in the qRT-PCR analysis. Primers used were shown in Table S1.

RNA Degradation Assay

HEK293T cells were transfected with different expression vectors. Thirty hours post-transfection, cells were incubated with culture medium containing 5 μM of actinomycin D [37]. Cells were harvested at 0, 6, 12, 18, 24, and 30 h post-

actinomycin D treatment, and RNA was extracted. BAF155 mRNA levels were analyzed via qRT-PCR. The basal expression level of BAF155 mRNA at 0 h point of actinomycin D treatment of each condition was considered as 100%, regardless of the baseline changes in gene expression between two conditions. The relative level of BAF155 mRNA in % from each time point was calculated.

In Utero Electroporation

In utero electroporation was performed as described previously [57]. In the knockdown experiments shown in Fig. 4, an eGFP plasmid was co-injected with shRBM15 or EV at a concentration ratio of 1:4. In overexpression and rescue experiments as shown in Figs. 5 and 6, RBM15 plasmids were co-injected with BAF155 or EV at a concentration ratio of 1:1.

Luciferase Assay

Plasmids-containing promoter regions (harboring PAX6 binding sites) of the candidate genes (Ssx2ip, Wnt5a, Fgfr1, Celsr1, Pdgfrb, Cdc42ep1, Cdc42ep4) and firefly-luciferase reporter were cloned as previously described [28]. Luciferase assay was performed as described previously [28]. Briefly, the firefly-luciferase–based reporter gene constructs and renilla expression vector were co-transfected into Neuro2A cells in a 24-well plate using Lipofectamine 2000 (Life Technologies). The different experimental groups received additional expression plasmids (CMV-EV, CMV-Pax6, CMV-BAF155, CMV-RBM15) as indicated. Cell extracts were prepared after 48 h and assayed for luciferase activity with the use of a Dual-Luciferase Reporter Assay System (Promega) following manufacturer's protocol. In all cases, the firefly-luciferase–based reporter gene activity was normalized to the renilla control.

Western Blot, Immunohistochemistry

WB and IHC experiments were carried out as previously described [1, 58]. All the primary antibodies used in Western blotting are in 1:1000 dilution.

Imaging, Quantification, and Statistical Analyses

Images were captured using Axio Imager M2 (Zeiss) with a Neurolucida system and confocal fluorescence microscopy (TCS SP5; Leica). Images were further processed with Adobe Photoshop. IHC signal intensities were quantified by using ImageJ software, as described previously [1, 57]. Statistical comparisons were carried out using Student's *t* test and one-way ANOVA followed by Bonferroni's multiple comparison test where appropriate. The results are presented as means ± SEM. All details of statistical analyses for histological experiments are presented in Table S2.

Acknowledgments We acknowledge Dr. Francois Guillemot, Dr. Diane S. Krause, Dr. Rho H. Seong, and Dr. Hongjun Song for providing reagents. This work was supported by the Research Program, Faculty of Medicine, Georg-August-University Goettingen (TT), TU432/1-1, TU432/3-1 DFG grants (TT), Schram-Stiftung (TT), and DFG-CNMPB (TT, JFS).

Author Contributions Y.X, R.C.H, G.S, L.P, J.R performed experiments and analyzed data; R.N contributed to luciferase assay; Y.X, T.T designed experiments; J.F.S provided research tools and contributed to discussions. The authors declare no competing financial interests.

Compliance with Ethical Standards

Conflict of Interest The authors declare that they have no competing interests.

References

1. Narayanan R, Pirouz M, Kerimoglu C, Pham L, Wagener RJ, Kiszka KA, Rosenbusch J, Seong RH et al (2015) Loss of BAF (mSWI/SNF) complexes causes global transcriptional and chromatin state changes in forebrain development. Cell Rep 13(9):1842–1854
2. Jung I, Sohn DH, Choi J, Kim JM, Jeon S, Seol JH, Seong RH (2012) SRG3/mBAF155 stabilizes the SWI/SNF-like BAF complex by blocking CHFR mediated ubiquitination and degradation of its major components. Biochem Biophys Res Commun 418(3):512–517
3. Chen J, Archer TK (2005) Regulating SWI/SNF subunit levels via protein-protein interactions and proteasomal degradation: BAF155 and BAF170 limit expression of BAF57. Mol Cell Biol 25(20):9016–9027
4. Phelan ML, Sif S, Narlikar GJ, Kingston RE (1999) Reconstitution of a core chromatin remodeling complex from SWI/SNF subunits. Mol Cell 3(2):247–253
5. Sohn DH, Lee KY, Lee C, Oh J, Chung H, Jeon SH, Seong RH (2007) SRG3 interacts directly with the major components of the SWI/SNF chromatin remodeling complex and protects them from proteasomal degradation. J Biol Chem 282(14):10614–10624
6. Nguyen H, Kerimoglu C, Pirouz M, Pham L, Kiszka KA, Sokpor G, Sakib MS, Rosenbusch J et al (2018) Epigenetic regulation by BAF complexes limits neural stem cell proliferation by suppressing Wnt signaling in late embryonic development. Stem Cell Reports 10(6):1734–1750
7. Nguyen H, Sokpor G, Pham L, Rosenbusch J, Stoykova A, Staiger JF, Tuoc T (2016) Epigenetic regulation by BAF (mSWI/SNF) chromatin remodeling complexes is indispensable for embryonic development. Cell Cycle 15(10):1317–1324
8. Bachmann C, Nguyen H, Rosenbusch J, Pham L, Rabe T, Patwa M, Sokpor G, Seong RH et al (2016) mSWI/SNF (BAF) complexes are indispensable for the neurogenesis and development of embryonic olfactory epithelium. PLoS Genet 12(9):e1006274
9. Ho L, Jothi R, Ronan JL, Cui K, Zhao K, Crabtree GR (2009) An embryonic stem cell chromatin remodeling complex, esBAF, is an essential component of the core pluripotency transcriptional network. Proc Natl Acad Sci U S A 106(13):5187–5191

10. Ho L, Ronan JL, Wu J, Staahl BT, Chen L, Kuo A, Lessard J, Nesvizhskii AI et al (2009) An embryonic stem cell chromatin remodeling complex, esBAF, is essential for embryonic stem cell self-renewal and pluripotency. Proc Natl Acad Sci U S A 106(13): 5181–5186
11. Panamarova M, Cox A, Wicher KB, Butler R, Bulgakova N, Jeon S, Rosen B, Seong RH et al (2016) The BAF chromatin remodelling complex is an epigenetic regulator of lineage specification in the early mouse embryo. Development 143(8):1271–1283
12. Schaniel C, Ang YS, Ratnakumar K, Cormier C, James T, Bernstein E, Lemischka IR, Paddison PJ (2009) Smarcc1/Baf155 couples self-renewal gene repression with changes in chromatin structure in mouse embryonic stem cells. Stem Cells 27(12):2979–2991
13. Tuoc TC, Narayanan R, Stoykova A (2013) BAF chromatin remodeling complex: cortical size regulation and beyond. Cell Cycle 12(18):2953–2959
14. Kim JK, Huh SO, Choi H, Lee KS, Shin D, Lee C, Nam JS, Kim H et al (2001) Srg3, a mouse homolog of yeast SWI3, is essential for early embryogenesis and involved in brain development. Mol Cell Biol 21(22):7787–7795
15. Han S, Choi H, Ko MG, Choi YI, Sohn DH, Kim JK, Shin D, Chung H et al (2001) Peripheral T cells become sensitive to glucocorticoid- and stress-induced apoptosis in transgenic mice overexpressing SRG3. J Immunol 167(2):805–810
16. DelBove J, Rosson G, Strobeck M, Chen J, Archer TK, Wang W, Knudsen ES, Weissman BE (2011) Identification of a core member of the SWI/SNF complex, BAF155/SMARCC1, as a human tumor suppressor gene. Epigenetics 6(12):1444–1453
17. Ahn J, Ko M, Lee C, Kim J, Yoon H, Seong RH (2011) Srg3, a mouse homolog of BAF155, is a novel p53 target and acts as a tumor suppressor by modulating p21(WAF1/CIP1) expression. Oncogene 30(4):445–456
18. Karakashev S, Zhu H, Wu S, Yokoyama Y, Bitler BG, Park PH, Lee JH, Kossenkov AV et al (2018) CARM1-expressing ovarian cancer depends on the histone methyltransferase EZH2 activity. Nat Commun 9(1):631
19. Wang L, Zhao Z, Meyer MB, Saha S, Yu M, Guo A, Wisinski KB, Huang W et al (2014) CARM1 methylates chromatin remodeling factor BAF155 to enhance tumor progression and metastasis. Cancer Cell 25(1):21–36
20. Decristofaro MF, Betz BL, Rorie CJ, Reisman DN, Wang W, Weissman BE (2001) Characterization of SWI/SNF protein expression in human breast cancer cell lines and other malignancies. J Cell Physiol 186(1):136–145
21. Kohashi K, Yamamoto H, Yamada Y, Kinoshita I, Taguchi T, Iwamoto Y, Oda Y (2018) SWI/SNF chromatin-remodeling complex status in SMARCB1/INI1-preserved epithelioid sarcoma. Am J Surg Pathol 42(3):312–318
22. Yan Z, Wang Z, Sharova L, Sharov AA, Ling C, Piao Y, Aiba K, Matoba R et al (2008) BAF250B-associated SWI/SNF chromatin-remodeling complex is required to maintain undifferentiated mouse embryonic stem cells. Stem Cells 26(5):1155–1165
23. Singhal N, Graumann J, Wu G, Araúzo-Bravo MJ, Han DW, Greber B, Gentile L, Mann M et al (2010) Chromatin-remodeling components of the BAF complex facilitate reprogramming. Cell 141(6):943–955
24. Kleger A, Mahaddalkar PU, Katz S–F, Lechel A, Joo JY, Loya K, Lin Q, Hartmann D et al (2012) Increased reprogramming capacity of mouse liver progenitor cells, compared with differentiated liver cells, requires the BAF complex. Gastroenterology 142(4):907–917
25. Jiang Z, Tang Y, Zhao X, Zhang M, Donovan DM, Tian X(C) (2015) Knockdown of Brm and Baf170, components of chromatin remodeling complex, facilitates reprogramming of somatic cells. Stem Cells Dev 24(19):2328–2336
26. Al Mutairi F et al (2018) A mendelian form of neural tube defect caused by a de novo null variant in SMARCC1 in an identical twin. Ann Neurol 83(2):433–436
27. Harmacek L, Watkins-Chow DE, Chen J, Jones KL, Pavan WJ, Salbaum JM, Niswander L (2014) A unique missense allele of BAF155, a core BAF chromatin remodeling complex protein, causes neural tube closure defects in mice. Dev Neurobiol 74(5): 483–497
28. Narayanan R et al (2018) *Chromatin remodeling BAF155 subunit regulates the genesis of basal progenitors in developing Cortex*. iScience 4:109–126
29. Tuoc TC, Boretius S, Sansom SN, Pitulescu ME, Frahm J, Livesey FJ, Stoykova A (2013) Chromatin regulation by BAF170 controls cerebral cortical size and thickness. Dev Cell 25(3):256–269
30. Meyer KD, Jaffrey SR (2017) Rethinking m(6)a readers, writers, and erasers. Annu Rev Cell Dev Biol 33:319–342
31. Liu J, Yue Y, Han D, Wang X, Fu Y, Zhang L, Jia G, Yu M et al (2014) A METTL3-METTL14 complex mediates mammalian nuclear RNA N6-adenosine methylation. Nat Chem Biol 10(2):93–95
32. Linder B, Grozhik AV, Olarerin-George AO, Meydan C, Mason CE, Jaffrey SR (2015) Single-nucleotide-resolution mapping of m6A and m6Am throughout the transcriptome. Nat Methods 12(8):767–772
33. Wang Y, Li Y, Yue M, Wang J, Kumar S, Wechsler-Reya RJ, Zhang Z, Ogawa Y et al (2018) N(6)-methyladenosine RNA modification regulates embryonic neural stem cell self-renewal through histone modifications. Nat Neurosci 21(2):195–206
34. Patil DP, Chen CK, Pickering BF, Chow A, Jackson C, Guttman M, Jaffrey SR (2016) M(6)a RNA methylation promotes XIST-mediated transcriptional repression. Nature 537(7620):369–373
35. Visel A, Thaller C, Eichele G GenePaint.org(2004) An atlas of gene expression patterns in the mouse embryo. Nucleic Acids Res 32(Database issue):D552–D556
36. Weng H, Huang H, Wu H, Qin X, Zhao BS, Dong L, Shi H, Skibbe J et al (2018) METTL14 inhibits hematopoietic stem/progenitor differentiation and promotes Leukemogenesis via mRNA m(6)a modification. Cell Stem Cell 22(2):191–205 e9
37. Lu DF, Wang YS, Li C, Wei GJ, Chen R, Dong DM, Yao M (2015) Actinomycin D inhibits cell proliferations and promotes apoptosis in osteosarcoma cells. Int J Clin Exp Med 8(2):1904–1911
38. Yoon KJ, Ringeling FR, Vissers C, Jacob F, Pokrass M, Jimenez-Cyrus D, Su Y, Kim NS et al (2017) Temporal control of mammalian cortical neurogenesis by m(6)a methylation. Cell 171(4):877–889 e17
39. Martinez-Martinez MA, De Juan Romero C, Fernández V, Cárdenas A, Götz M, Borrell V (2016) A restricted period for formation of outer subventricular zone defined by Cdh1 and Trnp1 levels. Nat Commun 7:11812
40. Tavano S, Taverna E, Kalebic N, Haffner C, Namba T, Dahl A, Wilsch-Bräuninger M, Paridaen JTML et al (2018) Insm1 induces neural progenitor delamination in developing neocortex via down-regulation of the adherens junction belt-specific protein Plekha7. Neuron 97(6):1299–1314 e8
41. Sokpor G, Castro-Hernandez R, Rosenbusch J, Staiger JF, Tuoc T (2018) ATP-dependent chromatin remodeling during cortical neurogenesis. Front Neurosci 12:226
42. Xiang Y, Laurent B, Hsu CH, Nachtergaele S, Lu Z, Sheng W, Xu C, Chen H et al (2017) RNA m(6)a methylation regulates the ultraviolet-induced DNA damage response. Nature 543(7646): 573–576
43. Engel M, Eggert C, Kaplick PM, Eder M, Röh S, Tietze L, Namendorf C, Arloth J et al (2018) The role of m(6)a/m-RNA methylation in stress response regulation. Neuron 99(2):389–403 e9
44. Koranda JL, Dore L, Shi H, Patel MJ, Vaasjo LO, Rao MN, Chen K, Lu Z et al (2018) Mettl14 is essential for epitranscriptomic regulation of striatal function and learning. Neuron 99(2):283–292 e5
45. Weng YL, Wang X, An R, Cassin J, Vissers C, Liu Y, Liu Y, Xu T et al (2018) Epitranscriptomic m(6)a regulation of axon

regeneration in the adult mammalian nervous system. Neuron 97(2):313–325 e6
46. Yoon KJ, Ming GL, Song H (2018) Epitranscriptomes in the adult mammalian brain: dynamic changes regulate behavior. Neuron 99(2):243–245
47. Wang P, Doxtader KA, Nam Y (2016) Structural basis for cooperative function of Mettl3 and Mettl14 methyltransferases. Mol Cell 63(2):306–317
48. Geula S, Moshitch-Moshkovitz S, Dominissini D, Mansour AA1, Kol N, Salmon-Divon M, Hershkovitz V, Peer E et al (2015) Stem cells. m6A mRNA methylation facilitates resolution of naïve pluripotency toward differentiation. Science 347(6225):1002–1006
49. Meng TG, Lu X, Guo L, Hou GM, Ma XS, Li QN, Huang L, Fan LH et al (2018) Mettl14 is required for mouse postimplantation development by facilitating epiblast maturation. FASEB J 33(1): 1179–1187
50. Fietz SA, Kelava I, Vogt J, Wilsch-Bräuninger M, Stenzel D, Fish JL, Corbeil D, Riehn A et al (2010) OSVZ progenitors of human and ferret neocortex are epithelial-like and expand by integrin signaling. Nat Neurosci 13(6):690–699
51. Hansen DV, Lui JH, Parker PRL, Kriegstein AR (2010) Neurogenic radial glia in the outer subventricular zone of human neocortex. Nature 464(7288):554–561
52. Wang X, Tsai JW, LaMonica B, Kriegstein AR (2011) A new subtype of progenitor cell in the mouse embryonic neocortex. Nat Neurosci 14(5):555–561
53. Betizeau M, Cortay V, Patti D, Pfister S, Gautier E, Bellemin-Ménard A, Afanassieff M, Huissoud C et al (2013) Precursor diversity and complexity of lineage relationships in the outer subventricular zone of the primate. Neuron 80(2):442–457
54. Florio M, Huttner WB (2014) Neural progenitors, neurogenesis and the evolution of the neocortex. Development 141(11):2182–2194
55. Farkas LM, Haffner C, Giger T, Khaitovich P, Nowick K, Birchmeier C, Pääbo S, Huttner WB (2008) Insulinoma-associated 1 has a panneurogenic role and promotes the generation and expansion of basal progenitors in the developing mouse neocortex. Neuron 60(1):40–55
56. Ma X, Renda MJ, Wang L, Cheng EC, Niu C, Morris SW, Chi AS, Krause DS (2007) Rbm15 modulates notch-induced transcriptional activation and affects myeloid differentiation. Mol Cell Biol 27(8): 3056–3064
57. Tuoc TC, Stoykova A (2008) Trim11 modulates the function of neurogenic transcription factor Pax6 through ubiquitin-proteosome system. Genes Dev 22(14):1972–1986
58. Tuoc TC, Radyushkin K, Tonchev AB, Pinon MC, Ashery-Padan R, Molnar Z, Davidoff MS, Stoykova A (2009) Selective cortical layering abnormalities and behavioral deficits in cortex-specific Pax6 knock-out mice. J Neurosci 29(26):8335–8349
59. Ping XL, Sun BF, Wang L, Xiao W, Yang X, Wang WJ, Adhikari S, Shi Y et al (2014) Mammalian WTAP is a regulatory subunit of the RNA N6-methyladenosine methyltransferase. Cell Res 24(2):177–189